Transmission through a nonlinear junction of photonic crystal waveguides

2008 J. Phys.: Condens. Matter 20 025202

(http://iopscience.iop.org/0953-8984/20/2/025202)

IOP PUBLISHING JOURNAL OF PHYSICS: CONDENSED MATTER

J. Phys.: Condens. Matter **20** (2008) 025202 (7pp) doi:10.1088/0953-8984/20/02/025202

Transmission through a nonlinear junction of photonic crystal waveguides

A R McGurn

Department of Physics, Western Michigan University, Kalamazoo, MI 49008, USA

E-mail: arthur.mcgurn@wmich.edu

Received 6 September 2007, in final form 5 November 2007
Published 6 December 2007
Online at stacks.iop.org/JPhysCM/20/025202

Abstract

The transmission characteristics of a junction of Kerr nonlinear optical media connecting three linear media photonic crystal waveguides is studied as a function of the nonlinearity of the junction media. The system treated and the difference equation approach used here were originally introduced by McGurn and Birkok (2004 *Phys. Rev.* B **69** 235105) where the focus was on showing the existence of intrinsic localized modes in the junction material. Here the conditions under which transmission resonances exist in the system are investigated as functions of the parameters characterizing the nonlinearity of the junction media. The patterns of resonant transmission peaks plotted in the parameter space of the nonlinearity are obtained and explained in terms of junction modes. The transmission resonances are seen to depend on the intrinsic localized modes, renormalized Fabry–Perot excitations, and other types of nonlinear excitations in the junction media. Some of the general features of the Kerr system results are compared with results from a simple junction system based on the logistic mapping.

1. Introduction

There is a long history of the study of patterns generated from nonlinear mappings [1–7]. Well known examples are patterns associated with chaos found in solutions of the logistic and other related mappings and the various attractors that characterize the dynamics of such systems [1–3]. From simple types of nonlinearity these systems produce complex patterns in their solutions that are unlike those found in linear mappings. Other types of patterns found in chemical and biological systems are the Turing patterns [1, 4–6]. Here the complexity in the pattern solutions arises from the interplay of the rate of diffusion and reactive transitions in various inhomogeneous processes. In more recent examples, Wolfram [7] shows that amazingly complex patterns are generated from small sets of short, compact, recursive rules. The complex behavior follows from the straightforward application of a simple rule over and over again. In all of these studies the common element is that fundamental changes in the dynamics of a system come from the introduction of very simple nonlinearities, even at the level of perturbations.

In this paper we look at a simple mapping or recursion relation from the study of the transmission of light through a waveguide junction of Kerr nonlinear media that joins three photonic crystal waveguides made of linear optical media [8–10]. In this system guided waves are incident on the junction from one waveguide and are transmitted into the two remaining waveguides. The object is to investigate the pattern of transmission resonances in the transmission coefficient computed as a function of the parameters characterizing the nonlinearity of the junction. The recursion relation considered was obtained in [11–13] where some of its properties were investigated. The system is based on a two-dimensional photonic crystal composed as a square lattice of infinite parallel axis dielectric cylinders and has a band structure consisting of sets of stop and pass bands for light moving in the plane of the lattice [14–17]. A waveguide is formed in the photonic crystal by cylinder replacement of a row of cylinders in the lattice with the replacement cylinders chosen so that a guided mode at a frequency in a stop band propagates in the plane of the lattice along the row of waveguide cylinders [7–12, 15–21]. The junction we study connects three semi-infinite waveguides. It has a center site and a few sites along each waveguide formed from Kerr nonlinear media [22–24]. (Here the nonlinearity is only in the junction material.) The transmission through the junction is studied in the parameter space describing the dielectric properties of the Kerr material [8–10, 13, 14, 22–26].

The object of the study is to determine the peaks in the transmission coefficient through the junction, to find their origins, to classify the patterns that arise in the peak

distribution when presented as functions of the parameters describing the Kerr nonlinear media, and to associate these peaks with various resonant excitations. Of particular interest will be the effects in the system of intrinsic localized modes, renormalized Fabry–Perot excitations, and other types of nonlinear modes of the junction.

In section 2, a brief review of the difference equation theory of the junction is given followed by discussions of the transmission coefficient patterns in the parameter space of the Kerr medium. The nature of the excitations in the junction at transmission resonances are discussed. A brief comparison is made with a simple junction model based on the logistic mapping. In section 3, general conclusions are presented.

2. Junction transmission

The transmission through a junction of Kerr nonlinear media joining three identical semi-infinite waveguides of linear dielectric is studied [8]. One waveguide contains the incident and reflected modes and the other two waveguides contain modes of equal intensity which are received as transmitted modes. The photonic crystal is a square lattice array in the x–y plane of parallel axis cylinders and the semi-infinite waveguides are along the positive x-, y-, and negative y-axes [8, 9, 12]. The junction consists of a central Kerr site at the origin of the x- and y-axes and first and second identical Kerr sites along the semi-infinite waveguides (see figure 1). The model was originally discussed in [8] and [9]. The waveguide and junction system is composed of replacement cylinders differing from the cylinders of the bulk photonic crystal through the addition of a small amount of dielectric material about the axes of each replacement cylinder. The electric field of the guided modes is separately constant over the added material in each replacement cylinder so that the electric fields at the centers of the replacement cylinders are related to one another by a set of difference equations. These equations allow for the solutions of the waveguide modes and the transmission coefficients through the Kerr junction [8]. For a detailed discussion of the origin of the difference equations the reader is referred to [11–13], and a brief outline of the discussions is also given in the appendix.

2.1. Review of the model equations

The waveguides and junction are characterized by a set of difference equations. For the semi-infinite channels, along the x-axis [8]

$$E_{n,0} = g_l[E_{n,0} + b(E_{n+1,0} + E_{n-1,0})] \tag{1}$$

for $n > 4$ and along the y-axis

$$E_{0,n} = g_l[E_{0,n} + b(E_{0,n-1} + E_{0,n+1})] \tag{2}$$

for $|n| > 4$. For the junction material

$$\begin{aligned} E_{0,0} = {} & g[(1+\lambda|E_{0,0}|^2)E_{0,0} \\ & + b(1+\lambda|E_{0,-1}|^2)E_{0,-1} + b(1+\lambda|E_{0,1}|^2)E_{0,1} \\ & + b(1+\lambda|E_{1,0}|^2)E_{1,0}], \end{aligned} \tag{3}$$

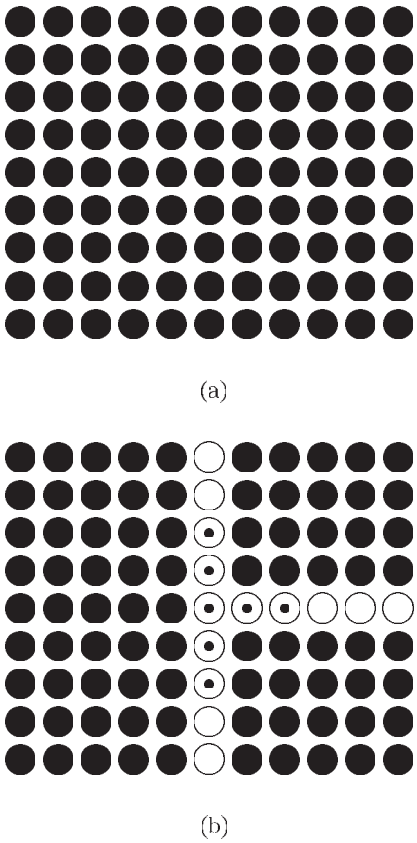

Figure 1. Schematic drawing of: (a) two-dimensional photonic crystal. The dielectric cylinders are perpendicular to the plane. The light moves in the plane and is polarized with the electric field parallel to the cylinder axes. (b) Photonic crystal waveguides meeting at a junction of Kerr nonlinear media. The open circles represent the linear media cylinders of the waveguide and the circles with the dot are the cylinders of the junction. The cylinders of the photonic crystal are represented by black circles.

$$\begin{aligned} E_{0,\pm1} = {} & g[(1+\lambda|E_{0,\pm1}|^2)E_{0,\pm1} + b(1+\lambda|E_{0,0}|^2)E_{0,0} \\ & + b(1+\lambda|E_{0,\pm2}|^2)E_{0,\pm2}], \end{aligned} \tag{4}$$

$$\begin{aligned} E_{1,0} = {} & g[(1+\lambda|E_{1,0}|^2)E_{1,0} + b(1+\lambda|E_{0,0}|^2)E_{0,0} \\ & + b(1+\lambda|E_{2,0}|^2)E_{2,0}], \end{aligned} \tag{5}$$

$$\begin{aligned} E_{0,\pm2} = {} & g[(1+\lambda|E_{0,\pm2}|^2)E_{0,\pm2} + b(1+\lambda|E_{0,\pm1}|^2)E_{0,\pm1}] \\ & + g_l b E_{0,\pm3}. \end{aligned} \tag{6}$$

$$\begin{aligned} E_{2,0} = {} & g[(1+\lambda|E_{2,0}|^2)E_{2,0} + b(1+\lambda|E_{1,0}|^2)E_{1,0}] \\ & + g_l b E_{3,0}, \end{aligned} \tag{7}$$

$$E_{0,\pm3} = g_l[E_{0,\pm3} + bE_{0,\pm4}] + gb(1+\lambda|E_{0,\pm2}|^2)E_{0,\pm2}, \tag{8}$$

and

$$E_{3,0} = g_l[E_{3,0} + bE_{4,0}] + gb(1+\lambda|E_{2,0}|^2)E_{2,0}. \tag{9}$$

Here $E_{m,j}$ is the electric field at the (m, j) lattice site which is polarized parallel to the cylinder axes, g_l characterizes the properties of the dielectric cylinders in the linear media waveguides, g and $\lambda \neq 0$ characterize the properties of the dielectric cylinders in the junction of Kerr media, and b is the coupling between the electric fields on nearest neighbor lattice sites of the waveguide. (See the appendix for more details

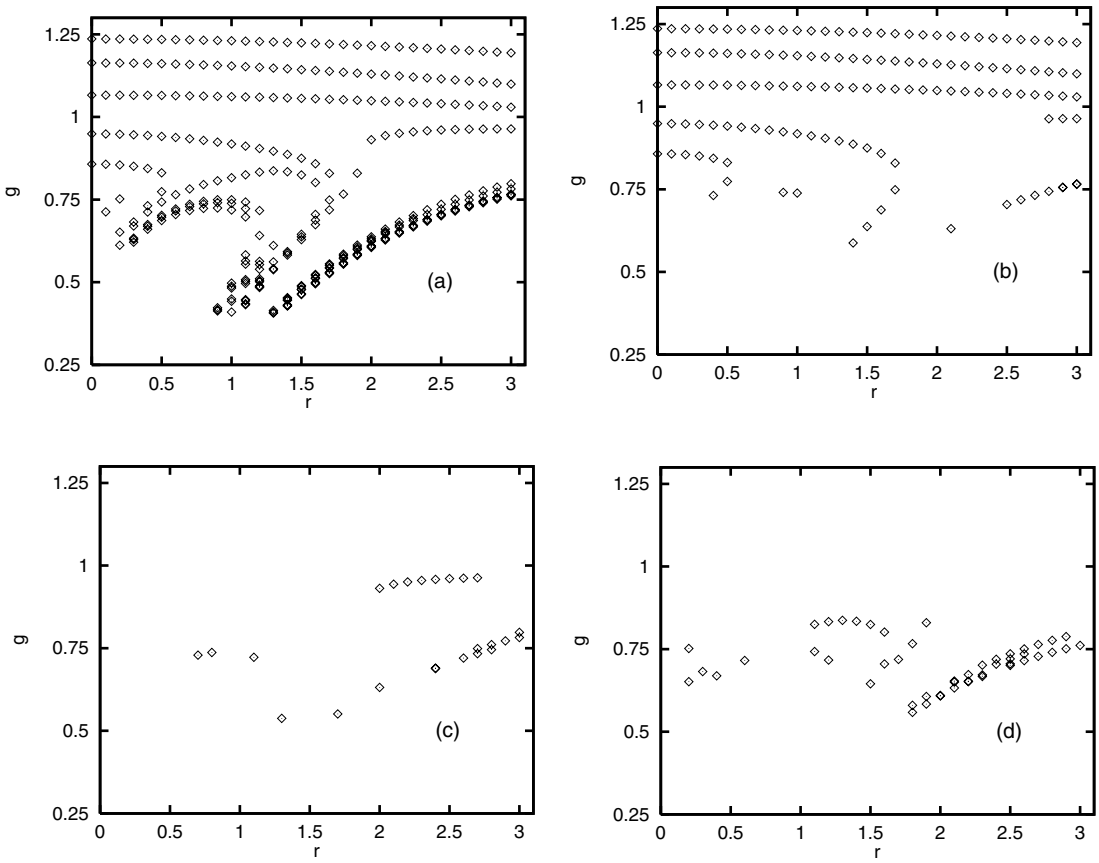

Figure 2. Plots of the peaks of the transmission coefficient, T, in the (r, g) plane. In: (a) peaks with $0.0 \leqslant T \leqslant 1.0$ are shown, (b) peaks with $0.6 \leqslant T \leqslant 1.0$ are shown, (c) peaks with $0.3 \leqslant T \leqslant 0.6$ are shown, and (d) peaks with $0.1 \leqslant T \leqslant 0.3$ are shown.

about the parameters. In particular, a detailed expression is given there for b in terms of Green's functions of the equations for the electric field modes of the photonic crystal and the dielectric constants of the waveguide and photonic crystal.)

The solutions in the transmitted mode linear media waveguides are of the form [8]

$$E_{0,n} = E_{n,0} = rx\mathrm{e}^{\mathrm{i}kn} \tag{10}$$

for $n > 2$ where r and x are real, and in the incident waveguide channel

$$E_{0,n} = u\mathrm{e}^{\mathrm{i}kn} + v\mathrm{e}^{-\mathrm{i}kn} \tag{11}$$

for $n < -2$. In the junction media the field at each site is a complex number satisfying the difference equations. The transmission coefficient is $T = 2|rx/u|^2$ which is obtained as a function of g and r for fixed λx^2. The solutions in the discussions below are made for parameters used in [8]. Specifically, $b = 0.0869$, $\lambda x^2 = 0.003$, $k = 3.1$, and $g_l = 1/(1 + 2b\cos(k))$.

2.2. Nonlinear transmission coefficient

The transmission coefficient, T, of the junction is studied as a function of the parameters of the nonlinear media. The transmission coefficient computed as a function of g for fixed r is found to be essentially a series of resonant transmission peaks [8]. In the limit that $r = 0$ the media in the junction is linear dielectric media, and the nonlinearity of the junction media increases as r increases from zero. In the following, discussions are given of the peaks found in the (r, g) parameter space, and these are associated with different types of junction excitations.

In figure 2 the position of peaks of T in the (r, g) plane are plotted. Figure 2(a) shows all peaks for $0.0 \leqslant T \leqslant 1.0$ and $g > 0.4$. The remaining subfigures present peaks in figure 2(b) for $0.6 \leqslant T \leqslant 1.0$, in figure 2(c) for $0.3 \leqslant T \leqslant 0.6$, and in figure 2(d) for $0.1 \leqslant T \leqslant 0.3$. The plots were made by computing the transmission coefficient as a function of g for a mesh of points along the r-axis and selecting out the maxima in T. These maxima are seen to cluster together into a pattern of different groups of features in the (r, g) plane, with the most significant peaks found for $g > 0.5$. Junction excitations of a given type are found to be held in common within a group of features. We now turn to a discussion of the excitations associated with different groupings in the (r, g) plane. Our focus will be on the large transmission peaks found in figure 2(b).

Figure 3 presents a number of plots for the junction wavefunctions at different (r, g) groupings. The modes of the junction of nonlinear media are displayed as $\lambda|E_{0,n}|^2$ versus $n = -2, -1, 0, 1, 2$, while results for the junction in the $\lambda = 0$ limit are given in terms of $|E_{0,n}|^2$ versus n.

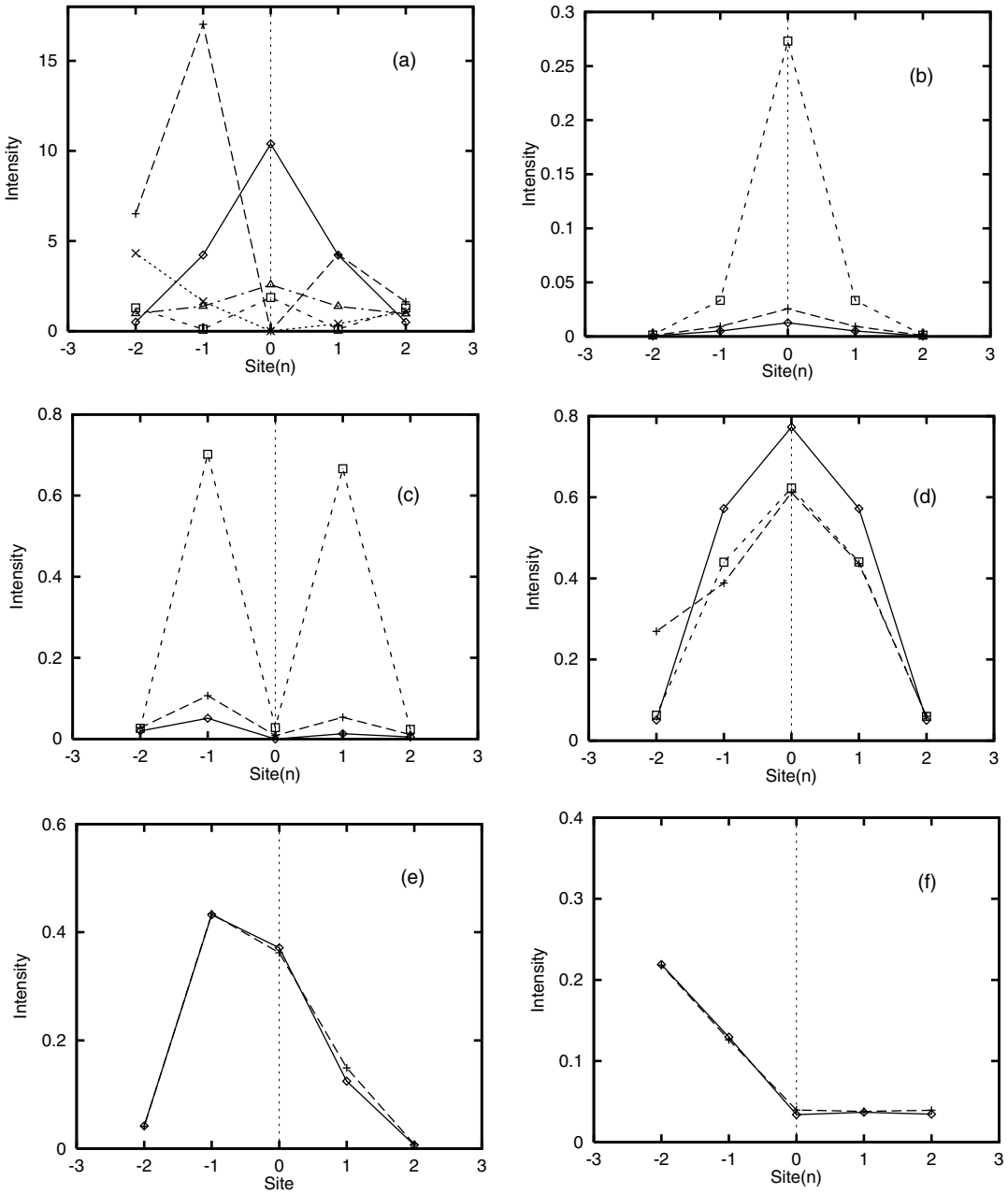

Figure 3. Plots of $\lambda|E_{0,n}|^2$ ($|E_{0,n}|^2$) versus n for the nonlinear (linear) media junction sites. In: (a) the linear media modes are shown for (0.0, 0.9490), (0.0, 0.8575), (0.0, 1.1635), (0.0, 1.2361), (0.0, 1.0661) from top to bottom at $n = -1$. (b) The modes for (0.4, 0.7314), (0.4, 0.8440), (0.1, 0.8568) are shown from top to bottom at $n = 0$. The mode at (0.1, 0.8568) is multiplied by 10. (c) The modes (1.4, 0.5878), (1.4, 0.8868), (0.1, 0.9487) from top to bottom at $n = 1$. The mode at (0.1, 0.9487) is multiplied by 100. (d) The modes (2.5, 0.7041), (3.0, 0.7651), (3.0, 0.7664) from top to bottom at $n = -1$. (e) The modes at (0.9, 0.7407) and (1.0, 0.7387) are shown. (f) The modes are (2.8, 0.9636) and (3.0, 0.9637) are shown. The lines in these plots are meant as a guide for the eyes. Note that in the $r = 0$ (linear) limit the absolute field amplitude has been taken as arbitrary as only the shape of the wavefunction is of interest. All values of (r, g) refer to figure 2(b).

Figure 3(a) show results for the $r = 0$ (linear media junction) limit. The guided modes resonate with five different Fabry–Perot-like modes of the junction. These resonances occur at $(r, g) = (0.0, 0.8575)$, $(0.0, 0.9490)$, $(0.0, 1.0661)$, $(0.0, 1.1635)$, and $(0.0, 1.2361)$. As r increases the system becomes nonlinear and modes evolving from $(0.0, 1.0661)$, $(0.0, 1.1635)$, $(0.0, 1.2361)$ extend across the top of figures 2(a) and (b) over the entire range of r. Along these three bands the nonlinear modes look similar to the linear modes they evolve from, but their amplitudes are fixed by the nonlinearity of the junction media and increase with increasing r. Bands of modes similar to those in the linear media limit also evolve from $(0.0, 0.9490)$, extending between $0.0 < r \leqslant 1.7$, and $(0.0, 0.8575)$, extending over $0.0 \leqslant r \leqslant 0.5$.

In figure 3(b) wavefunctions are shown for some of a ridge of modes found for $0.0 < r \leqslant 0.5$ and $0.73 < g < 0.86$. The modes are located at $(0.1, 0.8568)$, $(0.4, 0.8440)$, and

(0.4, 0.7314). Here the first two modes have small amplitudes and evolve from the linear mode at (0.0, 0.8575). The mode at (0.4, 0.7314), however, is an intrinsic localized mode, with an amplitude and shape that are fixed to a large extent by the Kerr nonlinearity of the junction media [8]. Using the theory in [9] this mode is associated with an intrinsic localized mode in a junction of semi-infinite Kerr nonlinear media waveguides. The intrinsic localized mode occurs at $g = 0.7435$ with amplitudes of $\lambda|E_{0,0}|^2 = 0.273$, $\lambda|E_{0,\pm1}|^2 = \lambda|E_{1,0}|^2 = 0.0431$, etc. (See [9] for the theory of intrinsic localized modes and the formulas giving the values of the intrinsic localized modes presented here.) It is important to note that the lower branch of the ridge is associated with intrinsic localized modes and this branch ends before the $r = 0$ axis.

Upon increasing the nonlinearity into the region $1.4 \leqslant r \leqslant 1.7$ another ridge of resonant modes is found at $0.58 \leqslant g \leqslant 0.95$. In figure 3(c) plots are shown of the nonlinear media wavefunctions for (1.4, 0.5878), (1.4, 0.8868), and (0.1, 0.9487). The mode at (1.4, 0.5878) can be thought of as an array of three intrinsic localized modes, each occurring in one of the nonlinear media junction leads. Each mode involves the generation of a significant nonlinearity in the junction so that the mode determines and is determined by the nonlinear contribution to the dielectric media. The amplitude of the fields in the linear media waveguides is much less than that at the peaks of the intrinsic localized modes. The remaining two modes, (0.1, 0.9487) and (1.4, 0.8868), have much smaller field amplitudes and are essentially versions of the linear mode at (0.0, 0.9490) that have been weakly renormalized by the Kerr nonlinearity. The branch containing the intrinsic localized modes is found to vanish for decreasing r before the $r = 0$ axis is reached.

Increasing the nonlinearity into the region $2.5 \leqslant r \leqslant 3.0$ and $0.7 < g < 0.8$ a further ridge of new modes is found. In figure 3(d) these modes are shown for (2.5, 0.7041), (3.0, 0.7664), and (3.0, 0.7651). The modes are much broader pulses than are those of the intrinsic localized modes and are of much greater peak amplitudes than those of the intrinsic localized modes. Again the fields at the peaks are much greater than the fields in the linear media waveguide and than those found in the previously discussed intrinsic localized modes. These modes might be thought of as broader localized pulses.

The modes in the remaining features in figure 2(b) are less easily characterized. Two modes are found in between the ridge of the intrinsic localized junction modes and the ridge of three intrinsic localized modes in the three junction leads. These occur at (0.9, 0.7407) and (1.0, 0.7387) and have wavefunctions plotted in figure 3(e). The modes are similar in structure, exhibiting large nonlinearities within the barrier generated by the small fields in the three semi-infinite waveguides. The fields are more evenly spread between the three junctions in a broad peak centered in the input lead of the junction and comparatively large fields are formed in the junction media by the much smaller fields in the linear media waveguides. In addition, a branch of modes in found containing modes at (2.8, 0.9636) and (3.0, 0.9637). Plots of these modes are given in figure 3(f). It is seen the these modes are formed as an interpolation between the boundary conditions set by the incident and transmitted waveguide modes. Here the field amplitude of the incident mode must be as large as the field amplitude at the left hand edge of the barrier material.

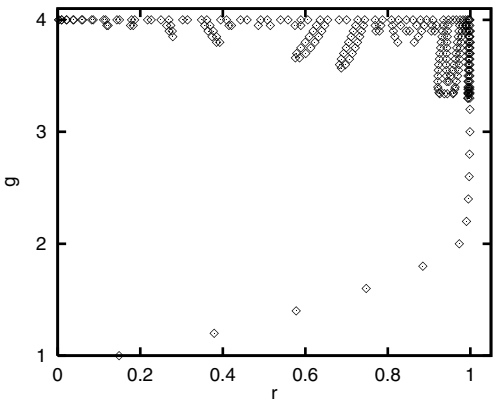

Figure 4. Plot of regions of $r_{0,-3} = r_{0,3} + r_{3,0} = r$ in the (r, g) plane for the system based on the logistic mapping.

2.3. *Logistic mapping*

Similar types of behaviors to those in the Kerr media junction are found in a simple model based on the logistic mapping [2]. Using a junction geometry similar to that in figure 1(b), consider the junction defined by

$$r_{0,n+1} = g r_{0,n}[1 - r_{0,n}] \tag{12}$$

for $n = -3, -2, -1, 0, 1, 2$, and

$$r_{n+1,0} = g r_{n,0}[1 - r_{n,0}] \tag{13}$$

for $n = 0, 1, 2$ where the $r_{n,0}$ and $r_{0,n}$ are values of quantities associated with the $(n, 0)$ and $(0, n)$ lattice sites, respectively. Resonant transmission in this system is defined by the condition that the input $r_{0,-3} = r$ is equal to the sum of the outputs, i.e., $r_{0,3} + r_{3,0} = r$ where $r_{0,3} = r_{3,0}$. The behavior of the resulting resonant transmission solutions as plotted in the (r, g) plane is found to be quite similar to that in the plots of the transmission peaks in figure 2.

In figure 4 the transmission resonances are shown in the (r, g) plane for $0.0 < r \leqslant 1.0$ and $1.0 \leqslant g \leqslant 4.0$. These were computed for a discrete mesh in g. As in figure 2 the resonances cluster into a series of ridges, and the wavefunctions for points within the same ridge exhibit similar geometric properties. It is interesting to consider solutions that have small inputs, i.e., $r \ll 1$. These solutions are found to exhibit large intermediate peaks in the nonlinear media, arising from the nonlinearity. Such solutions are similar in this regards to intrinsic localized modes which depend on the nonlinearity of the system for their existence. A mode of this type exists for $(r, g) = (0.002\,35, 4.0)$ and its wavefunction is shown in figure 5(a). This is the smallest non-zero r giving a transmission resonance at $g = 4.0$. Another mode of interest is one which gives resonant transmission for the largest possible r. For $g = 4.0$ this occurs at $(0.999\,85, 4.0)$ and its

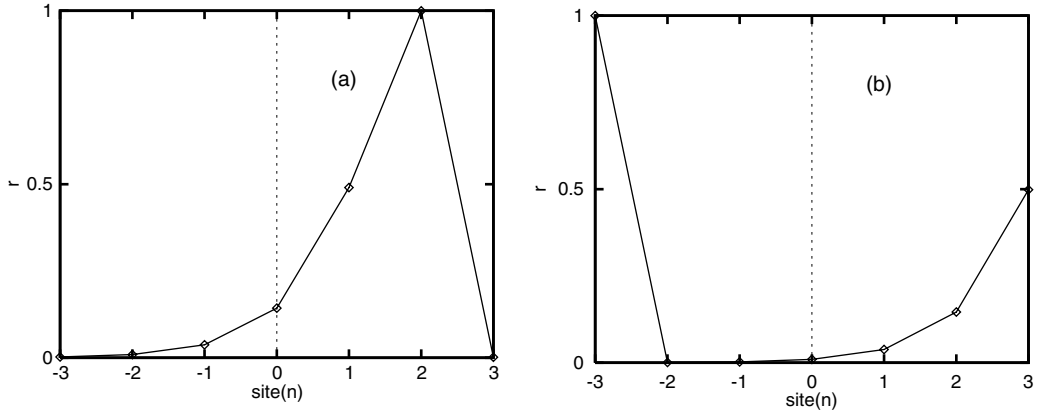

Figure 5. Plot of the wavefunction $r_{0,n}$ versus $n = -3, -2, -1, 0, 1, 2, 3$. Results are presented for: (a) (0.002 35, 4.0) and (b) (0.999 85, 4.0). The lines are meant as a guide for the eyes.

wavefunction shown in figure 5(b). The mode in figure 5(b) displays a geometric similarity to that found in figure 3(f) in a region of higher Kerr nonlinearities.

3. Conclusions

The transmission in a Kerr nonlinear junction has been studied as a function of the parameters characterizing the nonlinearity. It is found that: (1) The (r, g) plane has a patterning of transmission coefficient peaks that group into various ridges, and the different ridges can be identified with junction wavefunctions of a specific field geometry. The wavefunctions can be classified as evolving from the Fabry–Perot modes of the linear media system, various intrinsic localized modes whose generation is dependent on the nonlinearity, and other types of resonantly excited modes in the junction. (2) The intensity peaks for $0.60 \leqslant T \leqslant 1.0$ are most easily classified as in (1) and occur predominantly in the region $g > 0.6$. The peaks of smaller intensities often occur in the neighborhood of the $0.60 \leqslant T \leqslant 1.0$ peaks and have wavefunctions that are distortions of those of the $0.60 \leqslant T \leqslant 1.0$ peaks. Many smaller peaks are also found for $g < 0.6$. (3) Similar types of patterning to those found for the transmission coefficient in the (r, g) plane are found in the resonances of the logistic mapping in the (r, g) plane. In some cases roughly similar types of wavefunctions are found in both systems.

A comparison between the Kerr junction and logistic mapping results suggest that some of the common features observed in these system must be present in a wide variety of nonlinear mappings. This suggests that transmission studies such as those presented here should be effective in studying general excitations in a variety of nonlinear media. As in atomic, nuclear, and solid state systems an understanding of the physics of the system proceeds from an understanding of its variety of excitations. From the point of view of applications of nonlinear media in optics and electronics, however, most applications will rely on the understanding of nonlinear effects in small systems such as those treated here.

Appendix

A brief summary of the origin of the difference equation formulation is given here for the case in which the electric field of the modes is polarized with the electric field parallel to the axes of the dielectric cylinders. For more details the reader is referred to [11, 12], and [13].

The photonic crystal is described by a periodic dielectric function $\epsilon(\vec{x}_\parallel)$ where $\vec{x}_\parallel$ is in the plane of the Bravais lattice, perpendicular to the axes of the dielectric cylinders. A waveguide is defined by introducing a change in the dielectric constant, $\delta\epsilon(\vec{x}_\parallel)$, in a row of dielectric cylinders. Using the Helmholtz equation for the electric fields of the modes and standard methods of Green's functions, the electric fields of the waveguide modes satisfy [12, 13]

$$E(\vec{x}_\parallel) = \frac{\omega^2}{c^2} \int \mathrm{d}^2 x'_\parallel G(\vec{x}_\parallel, \vec{x}'_\parallel)\delta\epsilon(\vec{x}'_\parallel)E(\vec{x}'_\parallel). \qquad \text{(A.1)}$$

Here $G(\vec{x}_\parallel, \vec{x}'_\parallel)$ is the Green's function of the Helmholtz equations for the photonic crystal described by $\epsilon(\vec{x}_\parallel)$. If $\delta\epsilon(\vec{x}_\parallel)$ is non-zero only in a small region about the axes of cylinders forming the waveguide channel and $E(\vec{x}_\parallel)$ changes slowly over $\delta\epsilon(\vec{x}_\parallel)$ in each such cylinder, then equation (A.1) reduces (for a waveguide along the x-axis for which only on site and nearest neighbor site interactions are significant) to a set of difference equations given by

$$E_{n,0} = g_p[f_{n,0}E_{n,0} + b(f_{n+1,0}E_{n+1,0} + f_{n-1,0}E_{n-1,0})]. \qquad \text{(A.2)}$$

In equation (A.2), $f_{n,0} = 1 + \lambda|E_{n,0}|^2$ with $\lambda = 0$ for linear dielectric media, $g_p = \frac{\omega^2}{c^2}\int \mathrm{d}^2 x'_\parallel G(0, \vec{x}'_\parallel)\delta\epsilon(\vec{x}'_\parallel)$ where the integral is over the cylinder centered at $(0, 0)$, and $b = \int \mathrm{d}^2 x'_\parallel G(a_0\hat{i}, \vec{x}'_\parallel)\delta\epsilon(\vec{x}'_\parallel)/\int \mathrm{d}^2 x'_\parallel G(0, \vec{x}'_\parallel)\delta\epsilon(\vec{x}'_\parallel)$ where the integrals are computed as in the case of g_p and a_0 is the lattice constant of the waveguide. In the evaluation of all of the integrals in the definitions of g_p and b, $\lambda = 0$.

References

[1] Nicolis G and Prigogine I 1989 *Exploring Complexity* (New York: Freeman)
[2] Rasband S N 1990 *Chaotic Dynamics of Nonlinear Systems* (New York: Wiley)
[3] Puu T 2000 *Attractors, Bifurcations, and Chaos* (Berlin: Springer)
[4] Turing A M 1952 *Phil. Trans. R. Soc.* B **237** 37

[5] Rabinovich M I, Ezersky A B and Weidman P D 2000 *The Dynamics of Patterns* (Singapore: World Scientific)
[6] Koch A J and Meinhardt H 1994 *Rev. Mod. Phys.* **66** 1481
[7] Wolfram S 2002 *A New Kind of Science* (Urbana: Wolfram Media)
[8] McGurn A R and Birkok G 2004 *Phys. Rev.* B **69** 235105
[9] McGurn A R 2002 *Phys. Rev.* B **65** 75406
[10] McGurn A R 2003 *Chaos* **13** 754
[11] McGurn A R 1996 *Phys. Rev.* B **53** 7059
[12] McGurn A R 2000 *Phys. Rev.* B **61** 13235
[13] McGurn A R 1999 *Phys. Lett.* A **251** 322
[14] Phihal M, Shambrook A and Maradudin A A 1991 *Opt. Commun.* **80** 199
[15] Sakoda K 2001 *Optical Properties of Photonic Crystals* (Berlin: Springer)
[16] Joannopoulos J D, Villeneuve P R and Fan S 1995 *Photonic Crystals* (Princeton, NJ: Princeton University Press)
[17] McGurn A R 2002 *Survey of Semiconductor Physics* ed K W Boer (New York: Wiley) chapter 33
[18] Joannopoulos J D, Villeneuve P R and Fan S 1995 *Nature* **386** 143
[19] Favennec P N 2005 *Photonic Crystals: Toward Nanoscale Photonic Devices* (Berlin: Springer)
[20] McGurn A R 2007 *Complexity* **12** 18
[21] McGurn A R 2007 *Nonlinear Phenomena Research Perspectives* ed C W Wang (New York: Nova Science) chapter 8
[22] Mills D L 1998 *Nonlinear Optics* (Berlin: Springer)
[23] Boyd R W 2003 *Nonlinear Optics* 2nd edn (Amsterdam: Academic)
[24] Banerjee P P 2004 *Nonlinear Optics* (New York: Dekker)
[25] Kivshar Y S and Agrawal G P 2003 *Optical Solitons* (Amsterdam: Academic)
[26] McGurn A R 2004 *J. Phys.: Condens. Matter* **14** S5243